

Ultrahigh spontaneous emission quantum efficiency, 99.7% internally and 72% externally, from AlGaAs/GaAs/AlGaAs double heterostructures

I. Schnitzer, E. Yablonovitch, C. Caneau, and T. J. Gmitter

Bell Communications Research, Navesink Research Center, Red Bank, New Jersey 07701-7040

(Received 6 May 1992; accepted for publication 20 October 1992)

Optically thin AlGaAs/GaAs/AlGaAs double heterostructures, (5000 \AA), are floated off their substrates by the epitaxial liftoff technique and mounted on various high reflectivity surfaces. From the absolute photoluminescence intensity, we measure internal and external quantum efficiencies of 99.7% and 72%, respectively. High spontaneous emission quantum efficiency, is important for photon number squeezed light, diode lasers, single-mode light-emitting-diodes, optical interconnects, and solar cells.

In terms of luminescent quantum efficiency, at room temperature, the direct gap III-V semiconductors are rather unique substances. It has been known¹ for almost 20 yr that good quality III-V double heterostructures can have high internal quantum yields, well over 90% efficient. When combined with direct electrical injection, these high quantum yields form the basis for opto-electronics. This has led to important applications such as light-emitting diodes (LEDs), semiconductor lasers and solar cells, for each of which, the utmost quantum yield is desirable.

In this paper we will examine experimentally the absolute luminescent quantum yield of some good quality AlGaAs/GaAs/AlGaAs double heterostructures. We will find that the internal luminescent yield can be even higher than expected. Moreover, the high *internal* yield can be converted into an impressive *external* quantum efficiency by means of a simple geometrical configuration: III-V thin films are floated off their substrates by the epitaxial liftoff technique² and then mounted on various high reflectivity surfaces. We will show how this geometry allows most of the internal luminescence to escape externally, which can make LED efficiency competitive with the best laser diodes. In the race for low-threshold laser arrays, we consider such LEDs to be a significant development since they require *no* threshold current.

Some new developments in opto-electronics have put even greater emphasis on high quantum yields. Current-biased semiconductor lasers can produce a photon stream with sub-Poissonian shot noise,³ called photon number state squeezing. Likewise, there emerges a generation of light emitting devices sometimes referred to as zero-threshold lasers,⁴ but which are perhaps more accurately called single-mode light-emitting-diodes.⁵ In these types of devices, both the internal quantum efficiency, η , and the spontaneous emission factor, β , should be as close to unity as possible, where β is the fraction of spontaneous emission captured by the one desired electromagnetic cavity mode. Carrier injection noise is determined by $(1-\eta)$, while photon-number partition noise is measured by $(1-\beta)$. In this letter we will emphasize the highest possible internal and external quantum yield, η and η_{ext} , respectively.

In LEDs the external quantum efficiency is rather poor, generally only a few percent. The reason for this poor efficiency is that the semiconductor refractive index is

rather high, $n \sim 3.54$ in GaAs for example, leading to a very narrow escape cone for the isotropic spontaneous emission. The 16° cone angle imposed by Snell's Law covers a solid angle of only $\approx (1/4n^2) \times 4\pi$ steradians. Because the refractive index is so high, $4n^2 \approx 50$, the *external* efficiency is only $\approx 2\%$ in commonplace LEDs even when the *internal* efficiency happens to be close to unity. This problem has been addressed by incorporating a hemispherical semiconductor dome⁶ over the LED, allowing most of the internal luminescence to escape at normal incidence. We will show that semiconductor hemispheres are unnecessary and that a simple thin film geometry, as illustrated in Fig. 1, will also allow most of the light to escape externally.

A conventional n^+ -AlGaAs/ p -GaAs/ p^+ -AlGaAs double heterostructure is grown over a 500-\AA -thick AlAs release layer by organometallic chemical vapor deposition, where $n^+ \approx 3 \times 10^{18} \text{ cm}^{-3}$, $p \approx 3 \times 10^{17} \text{ cm}^{-3}$, and $p^+ \approx 3 \times 10^{18} \text{ cm}^{-3}$. The heterostructure is then separated from the GaAs substrate by epitaxial liftoff² (ELO), using HF acid selective etching of the AlAs release layer. Following the ELO procedure, the thin film, supported from above by a thick wax layer, is Van der Waals bonded by surface tension forces onto a reflecting substrate. As shown in Fig. 1, this substrate reflects the emitted photons back into the GaAs where they may be absorbed and possibly re-emitted into the escape cone. As a substrate we use high reflectivity metal mirrors coated with a low index transparent layer, which offers, when angle averaged, a higher effective reflectivity than a multilayer AlAs/GaAs Bragg reflector.⁵

Once a luminescent photon is emitted internally, it will have one of several possible destinies: (a) It can escape through the escape cone at the top of the double heterostructure; (b) it can be reabsorbed by the parasitic optical losses in the structure, in the bottom reflector for example; (c) it can be reabsorbed in the active layer and experience reincarnation as a photon. If there were no parasitic optical losses, and if the internal quantum efficiency, η , were high enough, the photon would be reincarnated many times, having a 2% probability of finding the escape cone each time. To achieve a high external quantum efficiency, as we have done, requires 25 or more reincarnations of the photon! This is illustrated in Fig. 2. Therefore, the external efficiency, η_{ext} , is a sensitive function of the small parasitic

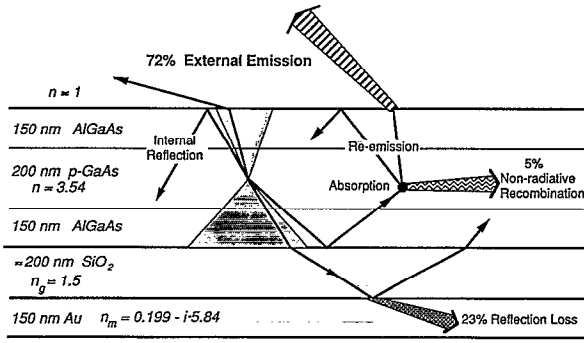


FIG. 1. Schematic cross section of epi-lift-off heterostructure, Van der Waals bonded onto an SiO₂ coated metallic reflector. The upper and lower escape cones are depicted by the shaded area. The partition among external emission, reflection loss, and nonradiative recombination processes, is indicated by percentages. Refractive indices are given by n , n_g , and n_m .

optical losses and the small nonradiative loss channel $(1-\eta)$.

To model the behavior of the photoluminescence in our GaAs films, we will invoke a statistical approach⁷ which was first introduced to explain the ergodic behavior of light in solar cells. We justify this statistical model by averaging over internal angle, polarization, over volume or the depth of luminescent material, over the wavelength band, and over thickness fluctuations or surface roughness. Therefore, coherent effects are ignored. Let B_{int} be the brightness (in photons/s per cm² per steradian) of the trapped luminescent radiation inside the thin film. The internal luminescence will generally be reabsorbed by surface absorption or volume absorption. The parasitic absorption at the surface of the reflector is

$$\int_0^{\pi/2} 2\pi B_{\text{int}} A [1-R(\theta)] \cos \theta \sin \theta d\theta = \frac{4\pi B_{\text{int}} A [1-\bar{R}]}{4}, \quad (1)$$

where θ is the polar angle, A is the surface area, and \bar{R} is the angle averaged reflectivity. The volume integrated absorption within the bulk is

$$\int \alpha(z) B_{\text{int}} dV d\Omega = 4\pi B_{\text{int}} A \sum_i \alpha_i d_i \quad (2)$$

where dV is the volume element, $d\Omega$ is the internal solid-angle element, $\alpha(z)$ is the local absorption coefficient and α_i and d_i are the absorptivity and thickness of the i th layer, respectively. The active layer reabsorbs radiation right at the band edge, while in the other layers there can be parasitic bulk absorption mechanisms. We assume one typical wavelength for each absorption coefficient α_i instead of a careful spectral averaging.

The band-to-band absorption in the active layer, α_0 , produces electron-hole pairs, which may be subdivided

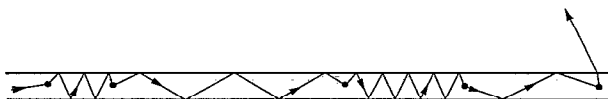


FIG. 2. Typical photon trajectory in the heterostructure shown in Fig. 1. Dots represent absorption/emission events. High external efficiency demands ~ 25 such events before a photon finds the escape cone.

into a portion $\eta\alpha_0$ which leads to reradiation and a portion $[1-\eta]\alpha_0$ which leads to nonradiative recombination and heat. The radiative part may itself be further subdivided into a fraction which falls within the forward or backward going escape cone, $2 \times (1/4n^2)$, and a remaining portion which rejoins the trapped internal radiation. Therefore, the internal bulk absorption in Eq. (2) may actually be divided into four terms: parasitic bulk absorption, band-to-band absorption leading to nonradiative recombination of electron-hole pairs, band edge absorption leading to external escape of the photons, and band edge absorption which contributes to the trapped pool of photons:

$$4\pi B_{\text{int}} A \left[\sum_j \alpha_j d_j + (1-\eta)\alpha_0 d_0 + \frac{\eta\alpha_0 d_0}{2n^2} + \eta\alpha_0 d_0 \left(1 - \frac{1}{2n^2}\right) \right], \quad (3)$$

where d_0 is the thickness of the active layer, and $\alpha_j d_j$ represents parasitic bulk absorption.

In steady state, the pump rate and the loss rates balance. The final term in Eq. (3), $\eta\alpha_0 d_0 (1 - 1/2n^2)$, is irrelevant since it merely represents re-emission into the pool of trapped luminescent photons and produces no net gain or loss. The external efficiency, η_{ext} , is the escape rate divided by the sum of all the rates in Eqs. (1) and (3):

$$\eta_{\text{ext}} = \frac{\eta\alpha_0 d_0 / 2n^2}{[\eta\alpha_0 d_0 / 2n^2 + (1-\eta)\alpha_0 d_0 + \sum_j \alpha_j d_j + (1-\bar{R})/4]}. \quad (4)$$

This may be further simplified by collecting all parasitic absorption into a loss term L representing the double pass parasitic absorption.

$$\eta_{\text{ext}} = \frac{\eta/2n^2}{[\eta/2n^2 + (1-\eta) + L/4\alpha_0 d_0]}, \quad (5)$$

where the double pass parasitic absorption is: $L \equiv (1-\bar{R}) + \sum 4\alpha_j d_j$.

The heterostructures were optically pumped using a continuous wave 780 nm AlGaAs laser, focused down to a 300 μm spot. Taking into account the laser power (15 mW), the pump photon energy, the Fresnel transmission into the heterostructure (68%), and the absorption fraction at the pump wavelength ($0.27 \leq A_p \leq 0.55$), we estimate the carrier injection rate to be equivalent to a current density between 2.5 A/cm² and 5 A/cm². This low level injection is nevertheless well into the radiative diffusion current regime (diode quality factor = 1) and about an order of magnitude above the recombination current dominated injection⁸ regime (diode quality factor = 2). We note that we are near the injection level at which highly efficient GaAs LEDs are expected to operate.

The luminescence was collected by an $f/0.3$ lens, focused through a pump-blocking 830-nm-long-wave-pass optical filter, and onto a biased Si photodiode. In all cases the photoluminescence signal was found to be linear in pump intensity (down to 20% of maximum intensity) as expected in our low-level-injection, but radiative diffusion current dominated, regime. Due to substantial statistical averaging under our experimental conditions a Lambertian angular distribution was always observed.

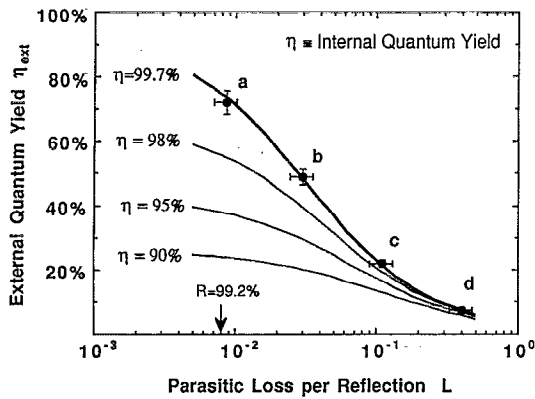


FIG. 3. The dependence of external quantum efficiency on double-pass parasitic optical absorption. The theoretical curves are plots of Eq. (5), with internal quantum yield as an adjustable parameter.

The absolute external quantum efficiency, η_{ext} , was measured by referencing the 880 nm photoluminescence signals to elastically scattered light at 780 nm from a white surface substituted for the sample in the identical optical setup. A minor correction was made for the difference in Si photodiode sensitivity between 780 and 880 nm wavelength. The signal ratio was then divided by the calculated pump absorption fraction to yield the true value for external quantum yield, η_{ext} .

In estimating the pump absorption we note that the $\text{Al}_{0.3}\text{Ga}_{0.7}\text{As}$ cladding layers are transparent at the pump wavelength, while the 200 nm p -GaAs active layer has an absorption coefficient^{9,10} of $\alpha_p = 1.5 \times 10^4 \text{ cm}^{-1}$. The sample absorption was calculated using a multiple reflection model which takes into account the reflectivity of the metallic substrate and that of the air/semiconductor interface at the 40° incidence angle. We determined a pump absorption fraction $A_p \approx 0.54$ for good reflectors, $A_p \approx 0.3$ on glass, and $A_p = 0.27$ on the wafer before ELO.

The four cases [Figs. 3(a)–3(d)] represent different parasitic optical absorption in the thin film structure:

In case (a), only the Au metallic reflector absorbs light. The $\text{Al}_{0.3}\text{Ga}_{0.7}\text{As}$ layers were intentionally left undoped to eliminate free-carrier absorption. We calculated the absorption using the complex refractive index¹¹ $n_m = 0.199 - 5.84i$ for the Au at 880 nm, near the luminescence wavelength. This would lead to an air–Au reflectivity $R(0) = 97.8\%$, and an SiO_2 –Au reflectivity $R(0) = 96.8\%$. The effective reflectivity is much higher however. Due to the narrow 25° escape cone entering the SiO_2 layer from the semiconductor, most of the light is totally internally reflected, and only a small portion actually suffers parasitic absorption in the metal. We calculate the angle and polarization averaged reflectivity to be $\bar{R} = 99.2\%$ for Fig. 1.

In case (b), the 150 nm $\text{Al}_{0.3}\text{Ga}_{0.7}\text{As}$ layers were doped to $3 \times 10^{18} \text{ cm}^{-3}$, as would be needed for electrical pumping. Assuming the free-carrier absorption cross-sections¹⁰ for electron and hole sum to $1.1 \times 10^{-16} \text{ cm}^2$, the additional double-pass parasitic optical loss is $L = 2\%$.

In case (c), an additional layer of GaAs, 40-nm thick, was added in Fig. 1 between the AlGaAs layer and the SiO_2 layer, intentionally for creating parasitic optical ab-

sorption. Since the 40-nm-thick GaAs layer was unpassivated on one side, rapid surface recombination ensured that all absorbed optical energy would degrade rapidly to heat. An averaged band edge⁹ absorption $\alpha_0 = 5 \times 10^3 \text{ cm}^{-1}$ was assumed for the luminescent wavelengths. This implied an additional double pass parasitic loss $L = 8\%$.

In case (d), a Palladium mirror was substituted for SiO_2 –Au mirror. The doped heterostructure, including the 40 nm GaAs dead layer, was Van der Waals bonded onto Pd, resulting¹² in a metallurgical reaction and a robust bond. The GaAs–Pd mirror had a measured reflectivity $R(0) = 70\%$, which when combined with the bulk losses resulted in a total double pass parasitic loss $L = 40\%$.

The curves in Fig. 3, external yield η_{ext} versus parasitic loss L , plot Eq. (5) with the internal yield η as a parameter. The best fit implies an internal quantum efficiency $\eta = 99.7\% \pm 0.2\%$. Therefore we can estimate a nonradiative minority carrier lifetime, which is 300 times longer than the radiative time. The internal rate of spontaneous emission is expressed as Bnp , where B is the electron-hole radiative coefficient and np is the product of electron and hole densities. B is most accurately determined by the Shockley–van Roosbroeck relation⁹ which gives¹³ $B = 13 \times 10^{-10} \text{ cm}^{-3} \text{ s}^{-1}$, considerably larger than the usually accepted value. At our doping level $p = 3 \times 10^{17} \text{ cm}^{-3}$, the internal spontaneous emission lifetime per electron is 2.6 ns. Therefore, the nonradiative electron lifetime is 0.85 μs , similar to recent measurements¹⁴ in moderately doped n -GaAs. This lifetime, and the internal efficiency it allows, is a tribute to the electronic quality of doped GaAs double heterostructures.

This work was partially sponsored by DARPA and ONR under Contract No. N0014-90-C-0048.

¹R. J. Nelson and R. G. Sobers, *J. Appl. Phys.* **49**, 6103 (1978).

²E. Yablonovitch, T. J. Gmitter, J. P. Harbison, and R. Bhat, *Appl. Phys. Lett.* **51**, 2222 (1987).

³Y. Yamamoto, S. Machida, and W. H. Richardson, *Science* **255**, 1219 (1992).

⁴T. Kobayashi, T. Segawa, A. Morimoto, and T. Sueta, Technical Digest of the 43rd Fall Meeting of the Japanese Applied Physics Society, Sept. 1982, Proceedings No. 29a-B-6 (in Japanese).

⁵E. F. Schubert, Y.-H. Wang, A. Y. Cho, L.-W. Tu, and G. J. Zydzik, *Appl. Phys. Lett.* **60**, 921 (1992).

⁶W. N. Carr and G. E. Pittman, *Appl. Phys. Lett.* **3**, 173 (1963).

⁷E. Yablonovitch, *J. Opt. Soc. Am.* **72**, 899 (1982); E. Yablonovitch and G. D. Cody, *IEEE Trans. Elec. Dev.* **ED-29**, 300 (1982).

⁸For our double heterostructures the cross-over point in injection level from diode quality factor = 2 to diode quality factor = 1 is estimated to be at $\lesssim 1 \text{ A/cm}^2$, relying on parameters from: E. Yablonovitch, T. J. Gmitter, and B. G. Bagley, *Appl. Phys. Lett.* **57**, 2241 (1990).

⁹J. I. Pankove, *Optical Processes in Semiconductors* (Prentice-Hall, Inc., Englewood Cliffs, NJ, 1971).

¹⁰H. C. Casey, Jr. and M. B. Panish, *Heterostructure Lasers* (Academic, New York, 1978).

¹¹M. A. Ordal, R. J. Bell, R. W. Alexander, L. L. Long, and M. R. Querry, *Appl. Opt.* **26**, 744 (1987).

¹²E. Yablonovitch, T. Sands, D. M. Hwang, I. Schnitzer, T. J. Gmitter, S. K. Shastry, D. S. Hill, and J. C. C. Fan, *Appl. Phys. Lett.* **59**, 3159 (1991).

¹³E. Yablonovitch, T. J. Gmitter, and R. Bhat, *Phys. Rev. Lett.* **61**, 2546 (1988).

¹⁴G. B. Lush, D. H. Levi, H. F. MacMillan, R. K. Ahrenkiel, M. R. Melloch, and M. S. Lundstrom, *Appl. Phys. Lett.* **61**, 2440 (1992).